STM JOURNALS

International Journal of
Molecular Biotechnological Research

Volume 1, Issue 1, 2023
January—June
DOI (Journal): *10.37591/IJMBR*

https://journals.stmjournals.com/ijmbr/

Research IJMBR

In Silico Drug Design for *Mycobacterium tuberculosis* and Development of Host–Pathogen Interaction Network and Molecular Docking Procedures

Keerthana S.[1,*]

Abstract

Objective: *A leading cause of illness is the contagious disease tuberculosis (TB), this infection with Mycobacterium tuberculosis complex (MTBC) particularly M. tuberculosis and M. africanum, is what causes tuberculosis. Diverse receptor proteins (mycobacterial proteins) with various 3D structures and functions were evaluated to access the multi-domain antimycobacterial action of ligands. The specific receptor proteins PDB ID: 3PTY, PDB ID: 4OW8, PDB ID: 5KWA, and PDB ID: 3ZXR, were opted for this study to determine the antimicrobial activity and general suppression of the target bacteria.* ***Method:*** *In this research, Arabinosyltransferase C (3PTY), protein kinase A (4OW8), Proteasomal ATPase (5KWA), and Glutamine synthetase (3ZXR) with 50 phytocompounds and their derivatives were nominated for determining the binding affinity with target proteins. This process was carried out computationally, proteins were generated from PDB, and phytocompounds were generated from PubChem. Purification of target proteins by BIOVIA for Molecular docking which is tendered by PyRx and visualization of the 3D structures of target proteins with ligands by BIOVIA. Physiological screening of ligands by ADMETlab 2.0 and generation of Ramachandran plots and Hydrophobicity by BIOVIA and PDBsum Generate.* ***Result:*** *In this study, after the experimental analysis with different bioinformatics tools and software, 13 bioactive ligands with the greatest satisfactory interaction properties were chosen from 50 that are docked with the four different target Mycobacterium proteins in this investigation.* ***Conclusion:*** *Using computational and bioinformatics methodologies, plant anti-MTB phytocompounds with specific combating activity against particular target proteins have been outlined, and the target protein with advantages associated has been discovered.*

Keywords: Contagious, diverse, suppression, purification, molecular docking, visualization, ADMET analysis

INTRODUCTION

Mycobacterium is a type of germ that is the most common complicated infection causing *Mycobacterium tuberculosis* and *Mycobacterium leprosy* (MT). *Mycobacterium tuberculosis* is the etiological agent of TB, which is disseminated by aerosol droplets from people who are actively infected. When a human inhales these aerosol droplets comprising the bacterium, the pathogen invades the lungs and is engulfed by macrophages in the alveoli, which results in an infection and the most recurrent consequence, impacting 94% of people, is chronic lung infectious disease [1].

The world's population is diseased by *Mycobacterium tuberculosis* in about a third of its populace. Examining the incident notifications to WHO and TB epidemiological studies enables us to examine the global tuberculosis scenario in 1990

*Author for Correspondence
Keerthana S.
E-mail: keerthanashyam15@gmail.com

[1]Student, Department of Biotechnology, M S Ramaiah University of Applied sciences, Bengaluru, Karnataka, India

Received Date: March 02, 2023
Accepted Date: March 16, 2023
Published Date: March 30, 2023

Citation: Keerthana S. In Silico Drug Design for *Mycobacterium tuberculosis* and Development of Host-Pathogen Interaction Network and Molecular Docking Procedures. International Journal of Molecular Biotechnological and Research. 2023;1(1): 1–19p.

and its current flows. The average number of cases documented annually over the past ten years must have ranged from 2.5 to 3.2 million in total, with population expansion more than reflecting a recent little decline in the prevalence rate. Although statistics on TB cases reported by WHO Member States illustrate the severity of the condition, data should be evaluated with care [2].

Human TB has a sophisticated pathophysiology that is nevertheless unexplained. For such MTBC to survive, there are numerous interactions and co-options amongst host factors and bacterial determinants. It remains debatable if MTBC uses granuloma development as a defensive or survival mechanism in hosts. However, to thrive within humans, MTBC species have devised a variety of defense mechanisms to circumvent host immunological assault [3].

In compliance with their rates of growth, the *Mycobacterium* genera may indeed be divided into two distinct groups which include rapid-growing and slow-growing *Mycobacteria*. For illustration, slow-growing mycobacteria like *Mycobacterium leprae*, *Mycobacterium tuberculosis*, and *Mycobacterium bovis* cause human and bovine tuberculosis, respectively. The effect of treatment on infectiousness, key components to reducing TB patients' contagiousness is timely diagnoses and efficient treatment. Adequate intervention should be administered, taking into consideration medication vulnerability, administration strategy, dosage, duration, adherence, and improved bioavailability [4].

Various kinds of specific receptors like mycobacterial proteins were looked at to reassess the multi-domain broad-spectrum antimicrobial activity of ligands.

The fundamental enzyme arabinosyltransferase C (PDB ID: 3PTY), is a representative of the enzyme class transferase and crucial for important biological activities. The transferase enzyme arabinosyltransferase C works on arabinose that is synthesized in the furanose form and is essential in the polymerization of arabinogalactan, a crucial component of the cell wall of *Mycobacterium*. EMB is used in combination with the anti-cell wall drugs isoniazid, pyrazinamide, and rifampin (rifampicin), which inhibit the formation of arabinogalactan and lipoarabinomannan (LAM) [5].

The prominent purpose of protein kinase A (PDB ID: 4OW8) serves in governing the dynamics and shape of the *Mycobacterium* cell is well acknowledged. During mycobacterial proliferation and infestations, this protein is dramatically upregulated. The extracytoplasmic domain of protein kinase A (PknA), a transmembrane protein, is tethered to the cytosolic intracellular kinase domain via a juxtamembrane. PknA phosphorylates a diverse range of proteins that are critical for the production of mycolic acid, cell division, and peptidoglycans and the *Mycobacterium* needs PknA to thrive and survive in vitro since it has been independently triggered. This plays an essential role in the mechanics and modulation of *Mycobacteria*'s cell shape and during explosive mycobacterial development and invasion, it is elevated [6].

Proteasomal ATPase (PDB ID: 5KWA) are regulatory proteases that may be detected in certain bacterial species and are ubiquitous in eukaryotes and archaea. For *Mycobacterium tuberculosis* (MTB) to infect humans fatally, the proteasome system is crucial. The proteasomal adenosine triphosphatase (ATPase) Mpa (PDB ID: 5KWA) which binds, unfolds, and transports protein substrates into the MTB proteasome core component for disintegration, is a significant aspect of the system [7].

Glucose synthetase (GS) enzyme has been selected as a potential therapeutic target due to its importance critical for the survival and proliferation of *Mycobacterium* TB. In actuality, *M. tuberculosis* (Mt) has four glutamine synthetase (GS) homologs, among which only the glnA1 gene product, is abundantly expressed and necessary for the growth of bacteria both in vitro *and in vivo.* Through producing a poly-L-glutamate-glutamine, Mt GS largely contributes to the formation of cell walls and nitrogen metabolism. The bacterial growth is inhibited by the irrevocable inhibitor of M. tuberculosis extracellular glutamine synthetase. A noticeable drop in the infectivity cell wall component poly-glutamate/glutamine is connected with growth inhibition [8].

In this study, 50 phytocompounds and their derivatives are synthesized to ascertain the pharmacological characteristics and therapeutic impact against four proteins. This involves molecular docking and further methodologies.

METHODOLOGY

Ligand Retrieval

The 50 structures from the phytochemical components among several plants in SDF format were retrieved from the PubChem database (*http://www.ncbi.nlm.nih.gov/pcc*) [9]. Also, PubChem ID and Canonical SMILES were retrieved from this database. Utilizing the BIOVIA Discovery Studio visualizer, the ligands' specified 2D structures in SDF format were transcribed into PDB format [10].

Preparation and Purification of Proteins

The first open-source resource in the biological sciences is the Protein Data Bank (PDB). It is the only global depository of experimentally determined 3D structures of biological macromolecules and their complexes. The RCSB Protein Data Bank (*https://www.rcsb.org/*) [11] makes the target proteins structures arabinosyltransferase C (PDB ID: 3PTY), protein kinase A (PDB ID: 4OW8), proteasomal ATPase (PDB ID: 5KWA) and glutamine synthetase (PDB ID: 3ZXR) essential for this study. An aspect of the protein preparation phase involves the OPLS 2005 force field serves to assign bond orders, hydrogenate all atoms, generate zero-bond orders for metals, eliminate water atoms from hetero groups that are larger than 5, optimize hydrogen bonds, conserve energy encountered by BIOVIA Discovery Studio to extract microscopic molecules and macromolecule systems, discovery studio is a collection of software. Advanced drug design and protein modeling research may indeed be executed using one unifying graphical interface for the depiction of plots and graphical data interpretation, this program provides a variety of consumers [12].

Characterization of Protein

The interfaces of proteins and nanoparticles cannot be identified based on hydrophobicity on a macroscale for instance by measuring contact angles. Such substrates require hydration water dynamics into consideration during assessing their molecular hydrophobicity which is accounted for by BIOVIA Discovery Studio. Research and cutting-edge simulations demonstrate that water density oscillations perform as such a gauge; fluctuations are amplified close to hydrophobic surfaces and quenched with greater surface hydrophilicity [13]. The primary chain conformation angles of the polypeptide chain of a protein molecule are represented by the Ramachandran plot. The revised Ramachandran plot web server includes multiple enhanced options for exhibiting the conformation angles in various locations, as reported in the study. There are additional options to depict the conformation angles in various secondary structural elements and areas within the browser and values in the plot are rendered by PDBsum Generate (*https://bio.tools/pdbsum_generate*) [14].

Molecular Docking Studies

To anticipate a potential binding posture with the target protein molecule, molecular docking studies were conducted on the natural structures of arabinosyltransferase C, protein kinase A, proteasomal ATPase, and glutamine synthetase, as well as 50 additional modified structures of phytocompounds (test ligand). PyRx is a computer program for computational drug discovery that can screen libraries of drugs against prospective therapeutic targets. This provides the capability for medicinal chemists to conduct virtual screening from any interface and supports researchers during every stage of the procedure, from data preparation through job completion and outcome analysis [15].

The molecular docking of 50 phytocompounds of a variety of plants utilizing an empirical force field and a Lamarckian genetic process, the PyRx software performs binding predictions across molecules of ligands and receptors. Leveraging a multitude of interactions, including H-bonds, ionic contacts, hydrophobic interactions, and van der Waal's forces which are interpreted in the CSV format (Comma Separated Values) the binding energy quantifies the binding affinity between target sites and functional groups of ligand molecules. The ligand production entails several stages that result in modification and

optimization of the structure, which are then retained as .pdbqt. The optimal binding complex for quartet target proteins was designated as the top three conformations with the lowest binding affinities for each. The docked ligand structures were exported as .pdb files, and the interaction was visualized in BIOVIA Discovery Studio—DS. These insights enable the visual interpretation of the docking method that was used to match the chosen ligands with the receptor proteins [16].

Visualization of Proteins

The structure visualization program BIOVIA Discovery Studio was employed to display the results of the docked structures from the virtual screening tool PyRx. Visualizing the target protein over the best-binding conformations was retrieved in.pdb format and displayed with BIOVIA Discovery Studio Visualizer, this ascertains if the target proteins work as therapeutic agents for *Mycobacterium tuberculosis*. Three-dimensional models and nonbonded interactions between the ligands and the amino acids in the binding pocket of the proteins were examined in this study [17].

ADMET Processing

An important facet of lead optimization for synthetic compounds is the high-throughput in vitro ADME (absorption, distribution, metabolism, and excretion) screening approach. HT-ADME screening often includes in vitro test suites to evaluate the qualities or liabilities of compounds, including physicochemical traits, toxicities, permeability, metabolism as well and drug-drug interactions. The pharmaceuticals with exceedingly high binding affinities undergo further testing using ADMET filters. Following this, the DS 3.5 ADMET procedures were used to calculate the solubility, absorption, plasma protein binding, CYP2D6 inhibition, Lipinksi, BBB, and hepatotoxicity was analyzed using an online server called ADMETlab 2.0 (*https://admetmesh.scbdd.com/*) [18].

RESULT

Retrieval of Ligands

Chemicals named phytocompounds are obtained from plants and their metabolites. A substantial percentage of the pharmaceuticals we utilize every day in contemporary medicine have their antecedents in phytocompounds. Phytocompounds provide intriguing therapeutics that may be both efficacious and safe in the face of increased susceptibility to all kinds of infections. A total of 50 phytochemicals were obtained from PubChem while 13 (Table 1) of those that met the structural requirements of the lowest binding affinities were chosen for further research to dock with the four designated proteins. Where three phytocompounds 2D structures out of 13 were re-docked against four proteins for visualization (Figure 1).

Table 1. PubChem ID, ligand name, canonical SMILES of top 13 phytocompounds.

PubChem ID	Ligand name	Canonical SMILES
101607489	Ent-Beyer-15-en-19-oic acid	CC12CCC3C4(CCCC(C4CCC3(C1)C=C2)(C)C(=O)O)C
2751795	Horminone	CC(C)C1=C(C2=C(C(=O)C1=O)C3(CCCC(C3CC2O)(C)C)C)O
11485584	Verbalactone	CCCCCC1CC(CC(=O)OC(CC(CC(=O)O1)O)CCCCC)O
5281879	5′-methoxyhydnocarpin	COC1=CC(=CC2=C1OC(C(O2)C3=CC(=C(C=C3)O)OC)CO)C4 =CC(=O)C5=C(C=C(C=C5O4)O)O
5471129	Icarin	CC1C(C(C(C(O1)OC2=C(OC3=C(C2=O)C(=CC(=C3CC=C(C)C) OC4C(C(C(C(O4)CO)O)O)O)O)C5=CC=C(C=C5)OC)O)O)O
5280443	Apigenin	C1=CC(=CC=C1C2=CC(=O)C3=C(C=C(C=C3O2)O)O)O
5281614	Fisetin	C1=CC(=C(C=C1C2=C(C(=O)C3=C(O2)C=C(C=C3)O)O)O)O
440735	Eriodictiol	C1C(OC2=CC(=CC(=C2C1=O)O)O)C3=CC(=C(C=C3)O)O
5280445	Luteolin	C1=CC(=C(C=C1C2=CC(=O)C3=C(C=C(C=C3O2)O)O)O)O
128861	Cyanidin	C1=CC(=C(C=C1C2=[O+]C3=CC(=CC(=C3C=C2O)O)O)O)O
5281605	Noroxylin	C1=CC=C(C=C1)C2=CC(=O)C3=C(O2)C=C(C(=C3O)O)O
5281607	Chrysin	C1=CC=C(C=C1)C2=CC(=O)C3=C(C=C(C=C3O2)O)O
636489	Guaianolide	CC1=C2C(C3C(C(C1)OC(=O)C(=C)C)C(=C)C(=O)O3)C(=CC2=O)C

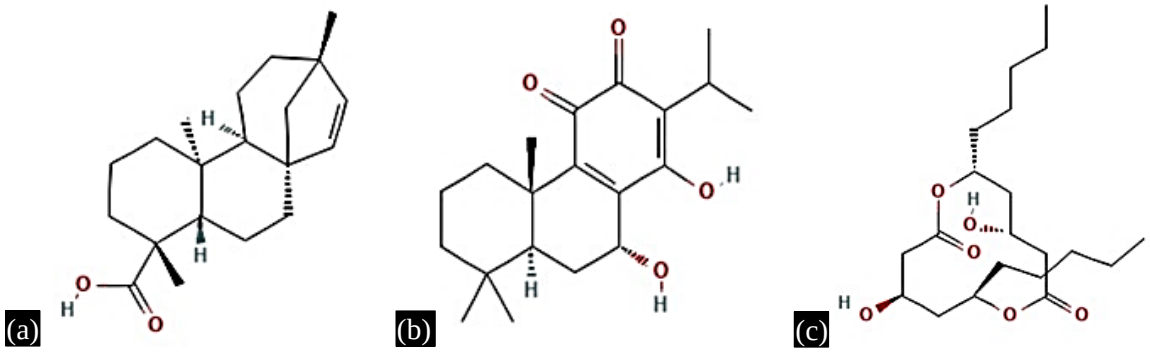

Figure 1. 2D structures of top 3 phytocompounds; (a) Ent-Beyer-15-en-19-oic acid, (b) horminone, and (c) verbalactone.

Structural Analysis of the Target Proteins

The four proteins that were taken from the PDB are purified in BIOVIA. Ramachandran plots, secondary structures, and hydrophobicity computations are all extracted from BIOVIA and PDBsum Generate, respectively, are depicted in Figures 2, 3, 4, and 5.

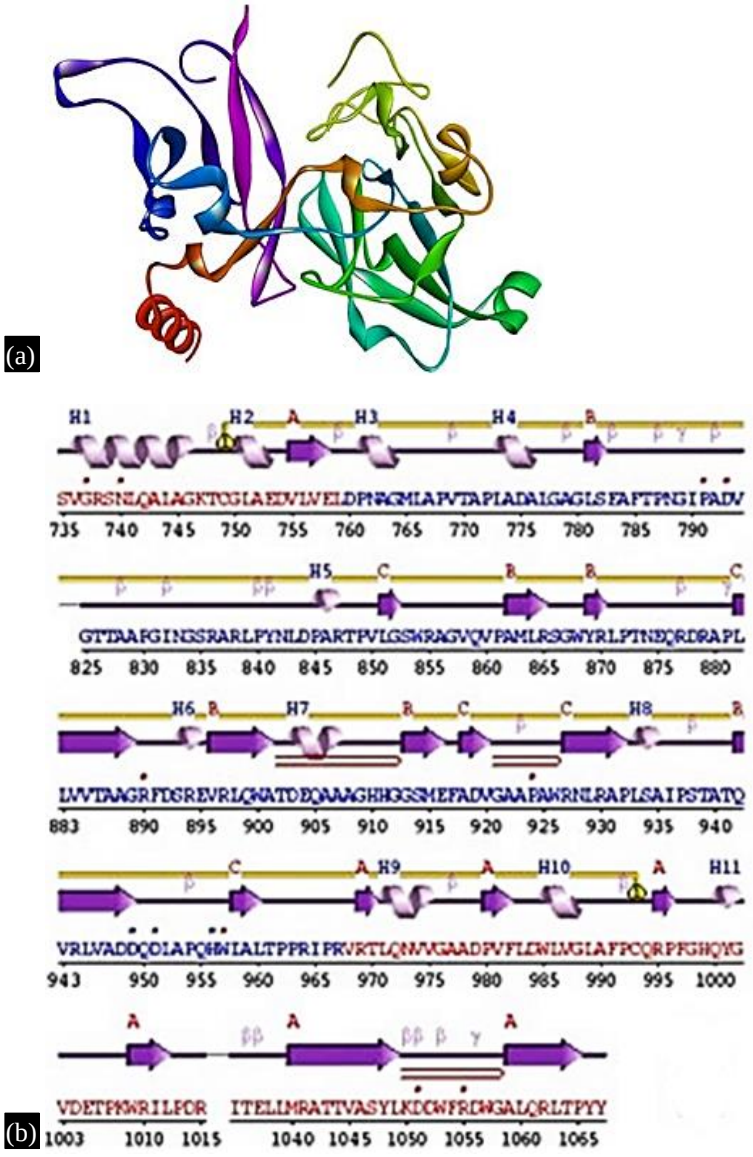

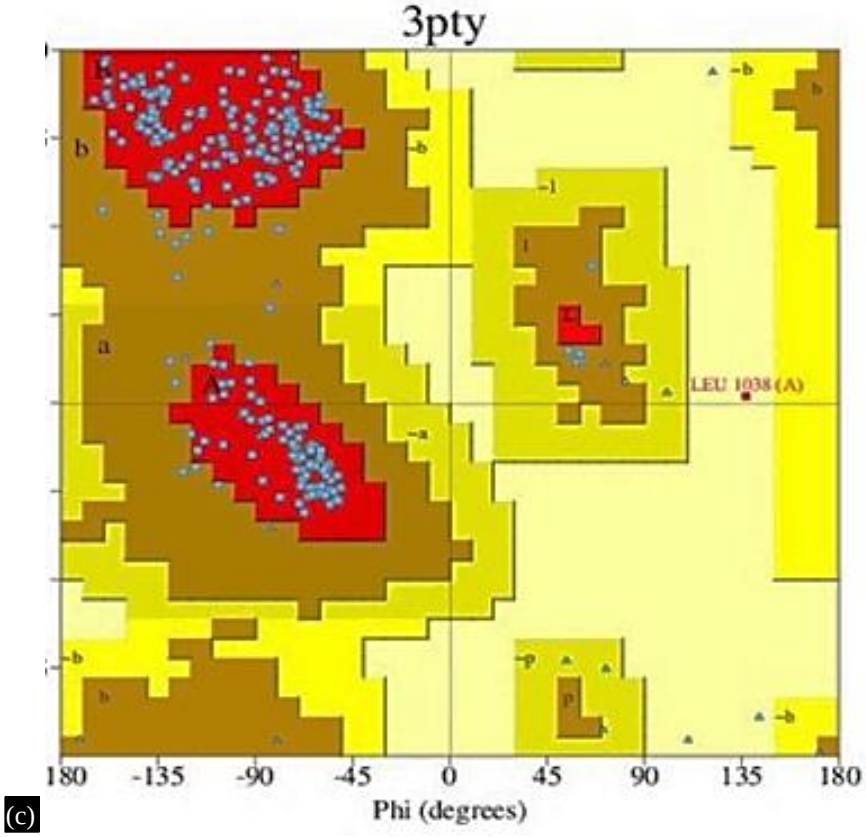

(c)

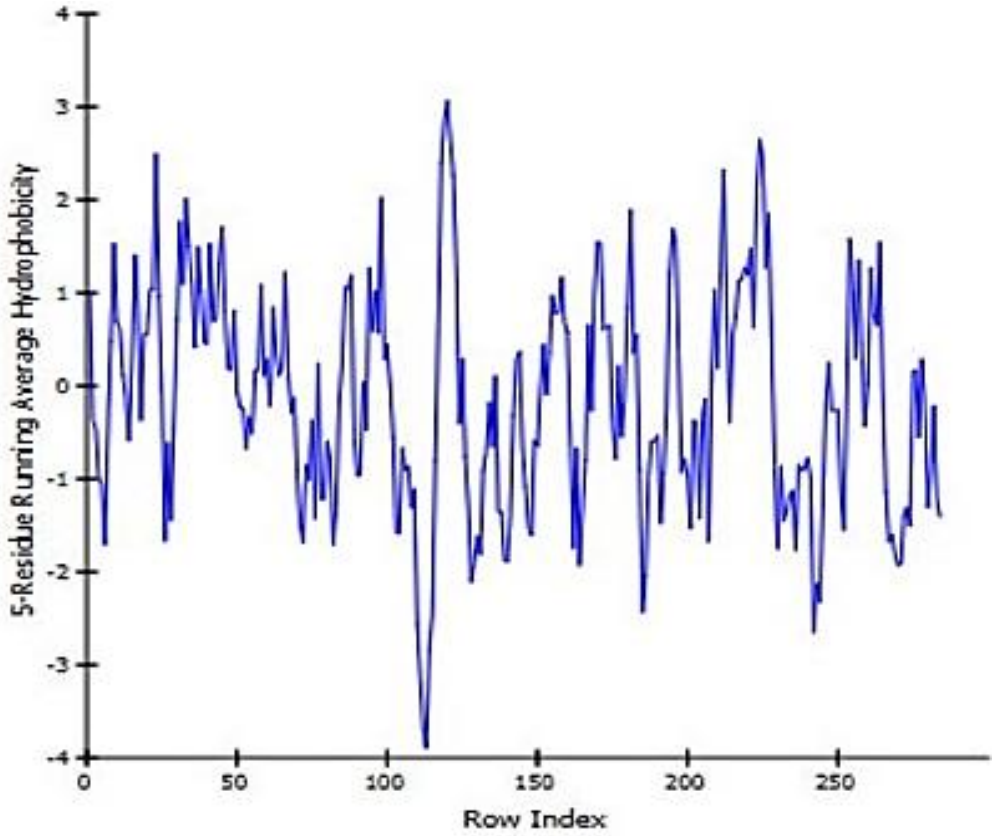

(d)

Figure 2. Structural analysis of 3PTY; (a) purified 3PTY protein, (b) secondary structure of 3PTY protein, (c) Ramachandran plot of 3PTY protein, (d) hydrophobicity plot of 3PTY protein.

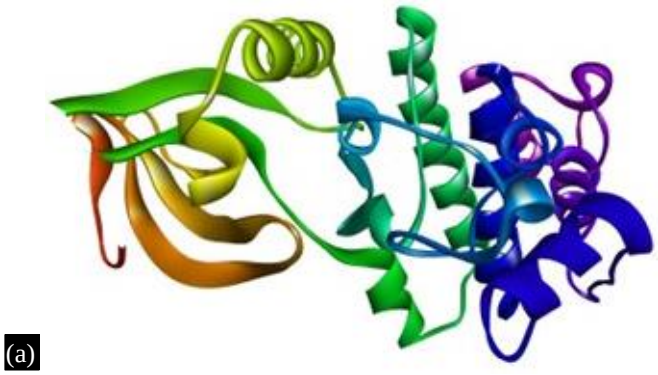

(a)

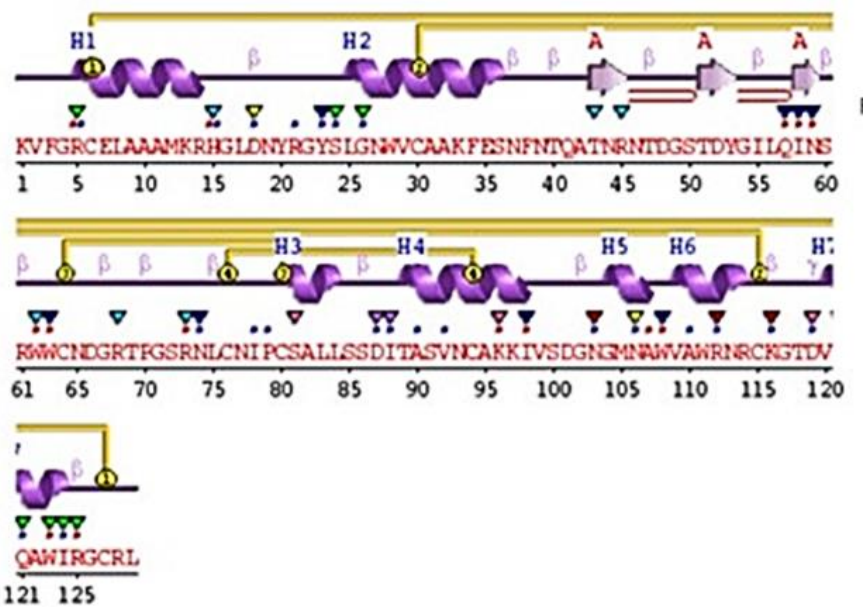

(b)

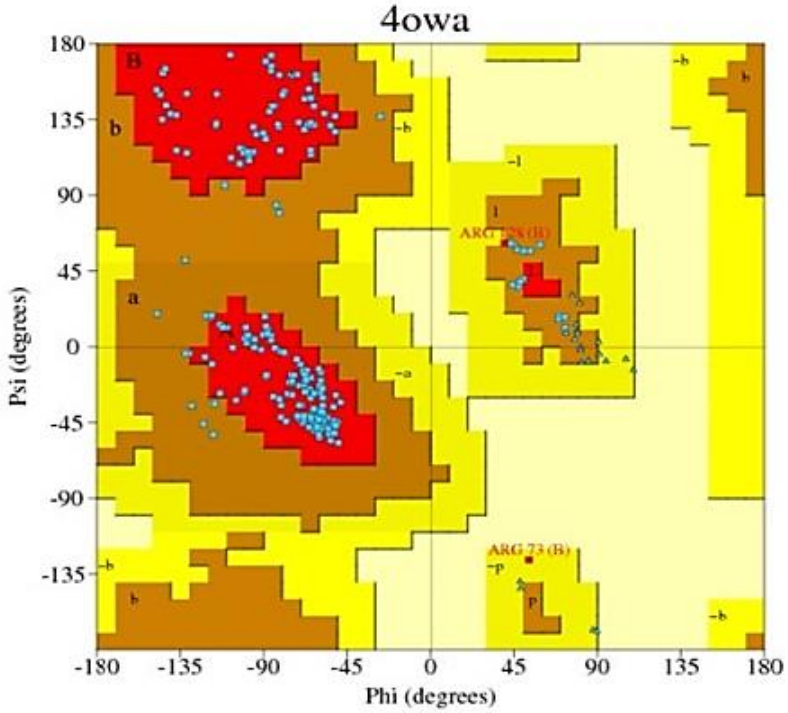

(c)

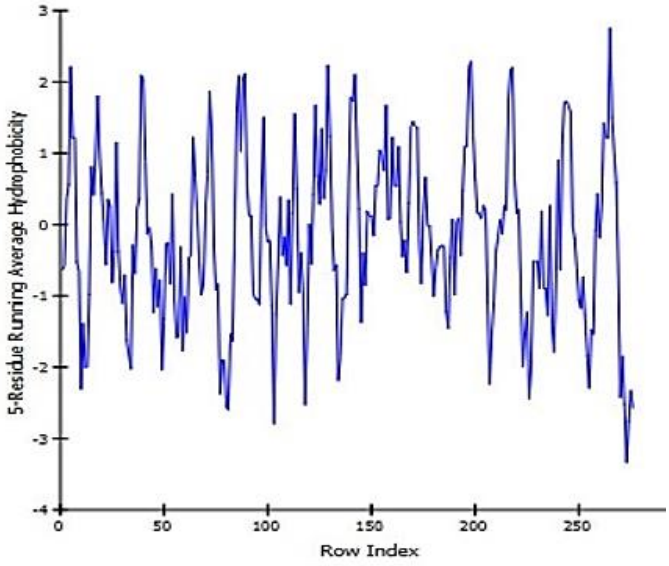

(d)

Figure 3. Structural analysis of 4OWA; (a) purified 4OWA protein, (b) secondary structure of 4OWA protein, (c) Ramachandran plot of 4OWA protein, (d) hydrophobicity plot of 4OWA protein.

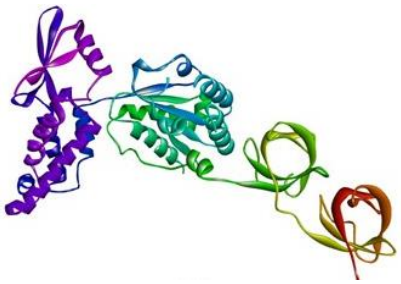

(a)

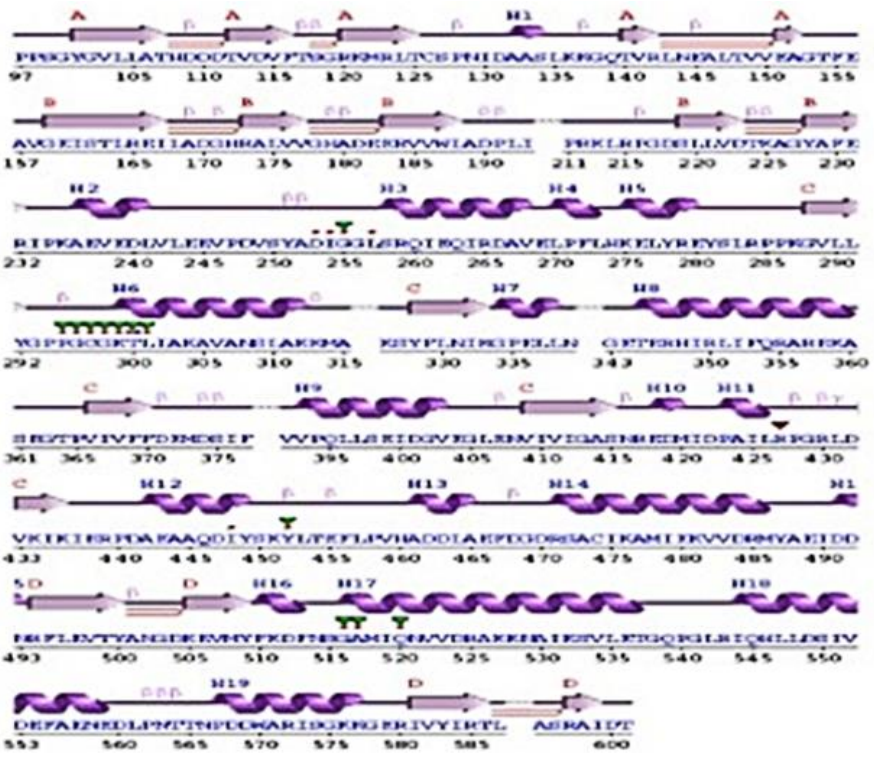

(b)

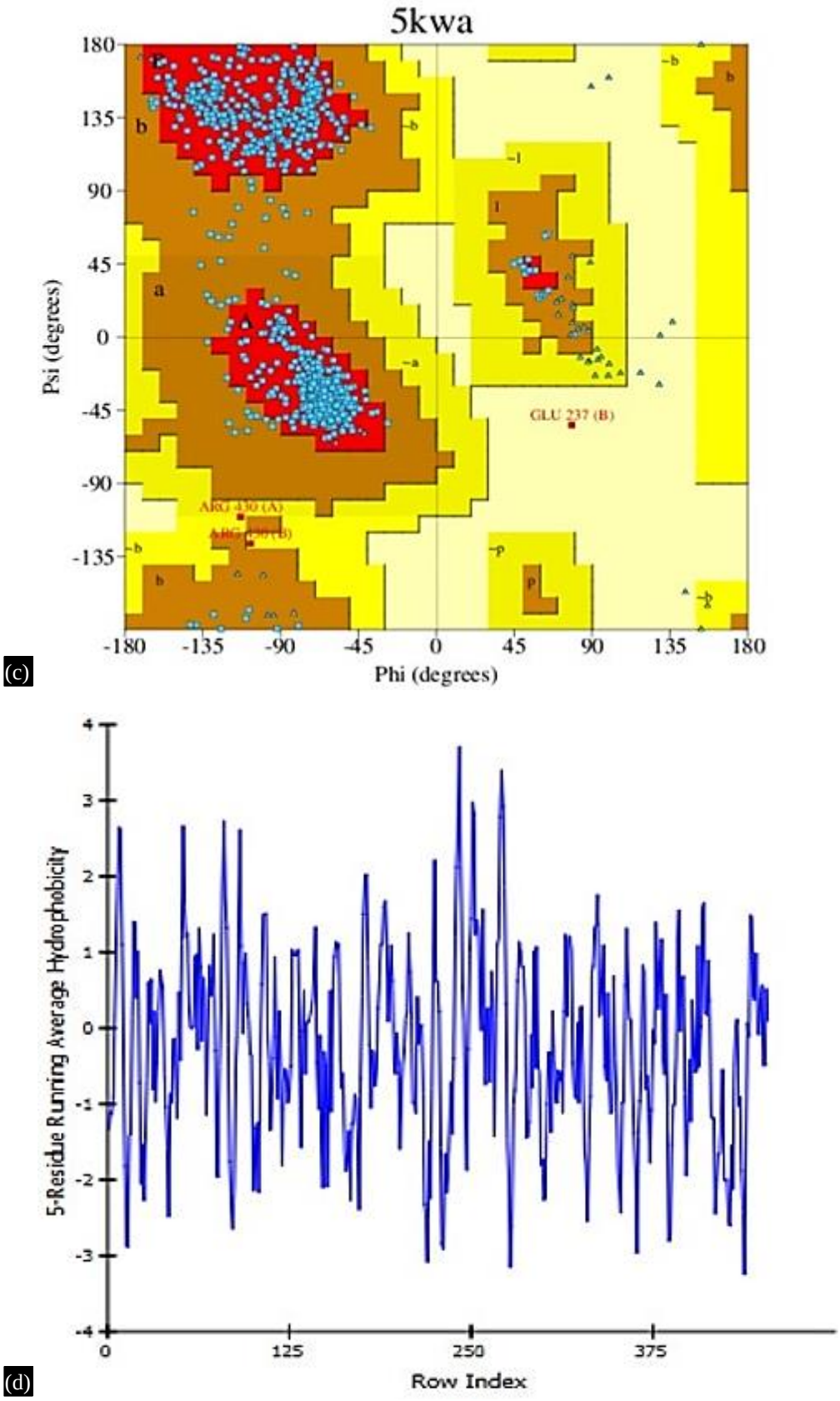

Figure 4. Structural analysis of 5KWA; (a) purified 5KWA protein, (b) secondary structure of 5KWA protein, (c) Ramachandran plot of 5KWA protein, (d) hydrophobicity plot of 5KWA protein.

(a)

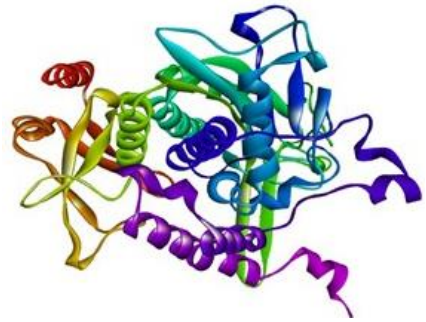

(b)

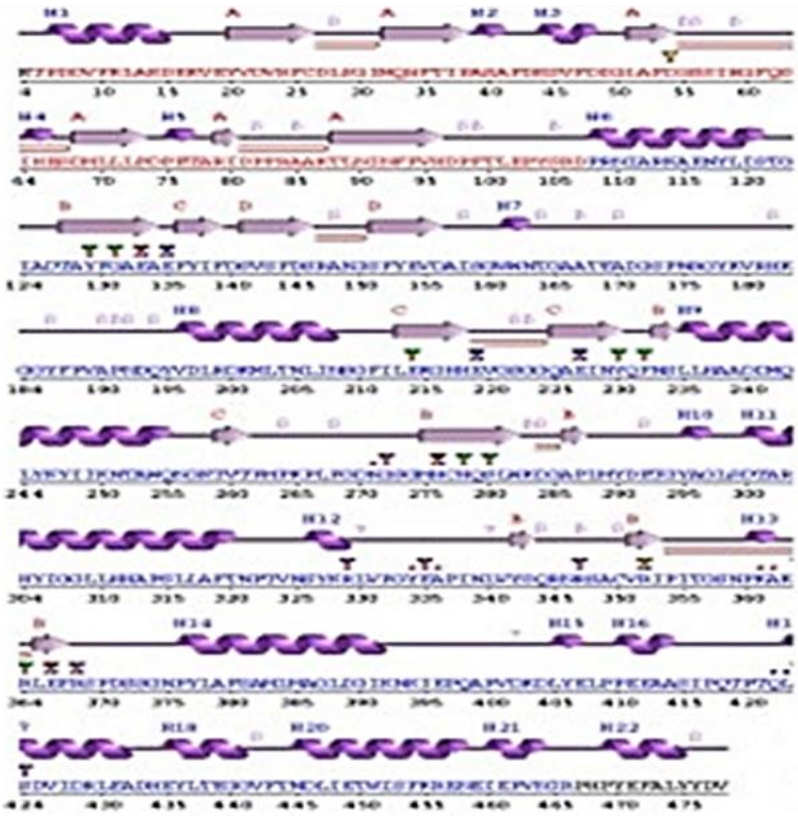

(c)

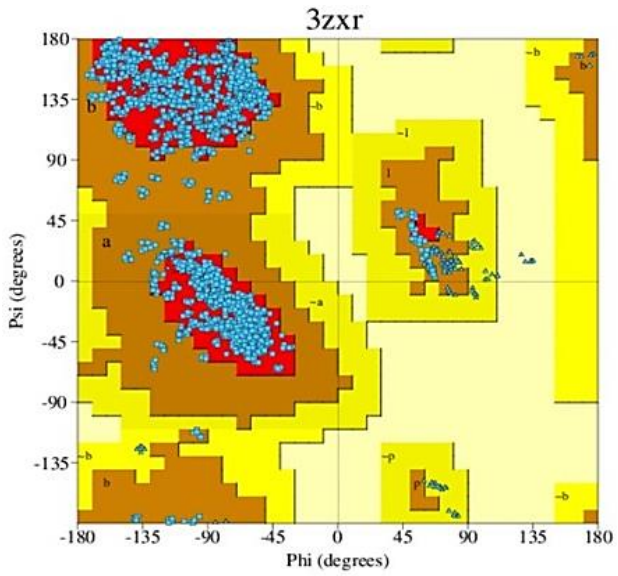

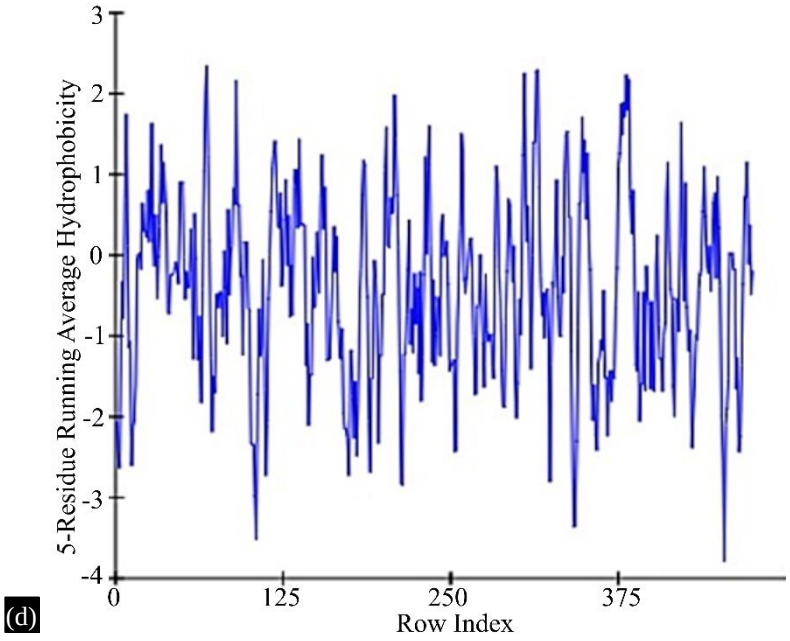

Figure 5. Structural analysis of 3XZR protein, (a) purified 3ZXR protein, (b) secondary structure 3ZXR protein, (c) Ramachandran plot of 3ZXR protein, (d) hydrophobicity plot of 3ZXR protein.

Ramachandran Plots and Their Statistics

The Ramachandran plots of the proteins with PDB ID: 3PTY, 4OWA, 5KWA, and 3ZXR were obtained using PDBsum Generate, as shown in Figures 2, 3, 4, and 5, respectively.

3PTY protein: According to the Ramachandran plot statistics the most favored regions[A, B, L] is 90.0%, additional allowed regions [a,b,l,p] is 9.5%, generously allowed regions [~a,~b,~l,~p] is 0.0%, the disallowed regions [XX] is 0.4%* and a total number of residues are 284.

4OWA protein: According to the Ramachandran plot statistics the most favored regions [A, B, L] is 87.6%*, additional allowed regions [a,b,l,p] is 11.5%, generously allowed regions [~a,~b,~l,~p] is 0.9%, the disallowed regions [XX] is 0.0 and a total number of residues are 258.

5KWA protein: According to the Ramachandran plot statistics the most favored regions [A, B, L] is 92.1%, Additional allowed regions [a,b,l,p] is 7.5%, generously allowed regions [~a,~b,~l,~p] is 0.3%, the disallowed regions [XX] is 0.1%* and a total number of residues are 908.

3ZXR protein: According to the Ramachandran plot statistics the Most favored regions [A, B, L] is 90.5%, additional allowed regions [a,b,l,p] is 9.5%, generously allowed regions [~a,~b,~l,~p] is 0.0%, the disallowed region [XX] is 0.0% and a total number of residues are 2850.

Hydrophobicity Plots

A peptide sequence's hydrophobicity could be seen along its whole length via hydropathy charts by BIOVIA Discovery Studio software. By using hydrophobic and hydrophilic attributes of the 20 amino acids, a hydropathy magnitude is employed. At each phase in the series, a rotating "window" calculates the hydropathy total. In this study, the hydrophobicity plots of the protein 3PTY, 4OWA, 5KWA, and 3ZXR are depicted in Figures 2, 3, 4, and 5, respectively.

Molecular Docking Results

In this article, a maximum of 50 phytocompounds were docked to four different *Mycobacterium* TB proteins of PDB ID: 3PTY, 4OWA, 5KWA, and 3ZXR out of 50 ligands, 13 were chosen for further

research having followed the preliminary evaluation and relying on their lowest binding affinities and root mean square deviation (RMSD) confirmation and again top 3 most satisfiable characteristics were chosen for visualization. Upon selection, the lowest binding affinity and RMSD were noted, and the top 13 ligands' binding affinities (BA) are summarized below [Table 2] namely *Ent-Beyer-15-en-19-oic acid* (PubChem ID: 101607489), *horminone* (PubChem ID: 2751795), *verbalactone* (PubChem ID: 11485584), *5'-methoxyhydnocarpin* (PubChem ID: 5281879), *icarin* 5(PubChem ID: 471129), *apigenin* (PubChem ID: 5280443), *fisetin* (PubChem ID: 5281614), *Eriodictiol* (PubChem ID: 440735), *luteolin* (PubChem ID: 5280445), *cyanidin* (PubChem ID: 128861), *noroxylin* (PubChem ID: 5281605), *chrysin* (PubChem ID: 5281607), *guaianolide* (PubChem ID: 5281607).

Table 2. The top 13 ligands PubChem ID and their binding affinities in target proteins.

Ligand PubChem ID	BA of 3PTY	BA of 40WA	BA of 5KWA	BA OF 3ZXR
101607489	-11.6	-11.5	-11.6	-13.7
2751795	-10.3	-11.7	-10.7	-13
11485584	-10.2	-10.5	-10.7	-12
5281879	-9.7	-9.4	-8.1	0
5471129	-9.4	-9.1	-8.3	0
5280443	0	-8.1	-7.7	-8.7
5281614	-8.2	0	-8.5	0
440735	-8.1	0	-7.9	0
5280445	-8.1	0	0	-8.7
128861	-8	0	0	-8.8
5281605	-8.1	0	0	-8.7
5281607	0	0	0	-9.1
636489	0	0	0	-8.9

Visualization Results

The top three ligands are exposed to visualization in the BIOVIA Discovery Studio tool to extract three-dimensional structures. These ligands possess common derivatives in all four target proteins. Likewise, statistics on the kind and classification of interaction as well as the bonding length for the appropriate residues of amino acids in the ligand were also inherited. The inherited 3D structures for the target proteins PDB ID: 3PTY, PDB ID: 4OWA, PDB ID; 5KWA, PDB ID: 3ZXR against three common ligands namely PubChem ID: 101607489, PubChem ID: 2751795, and PubChem ID: 11485584 (Figures 6, 7, 8, and 9).

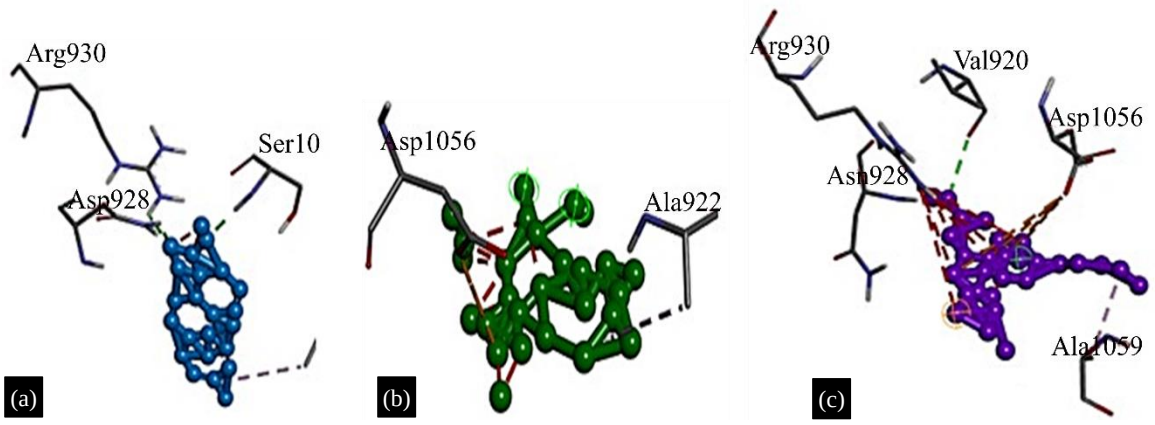

Figure 6. 3D interactions of ligands with protein PDB ID: 3PTY; (a) PubChem ID: 101607489, (b) PubChem ID: 2751795, (c) PubChem ID: 11485584, interacting with target protein of PDB ID: 3PTY.

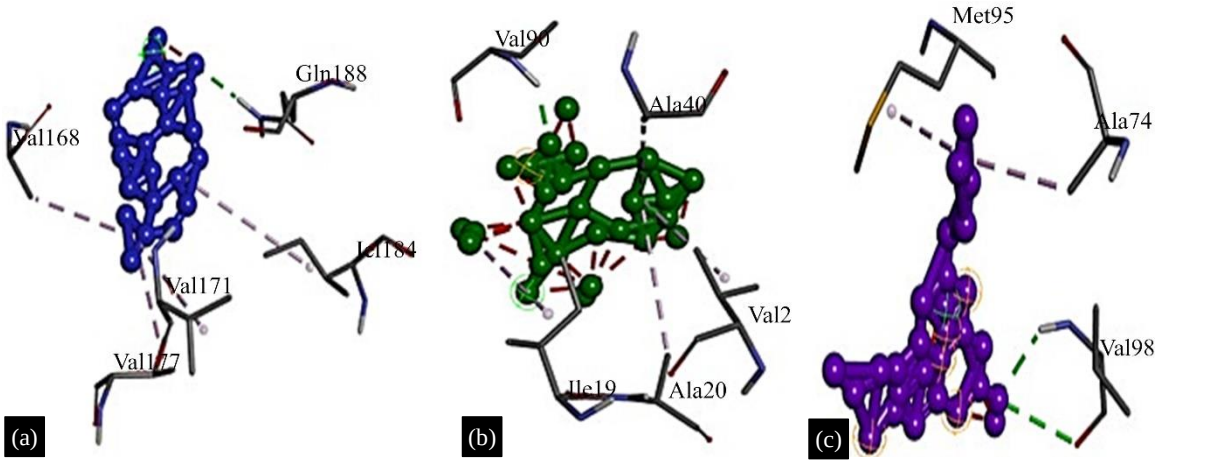

Figure 7. 3D interactions of ligands with protein PDB ID: 4OWA; (a) PubChem ID: 101607489, (b) PubChem ID: 2751795, (c) PubChem ID: 11485584 interacting with target protein of PDB ID: 4OWA.

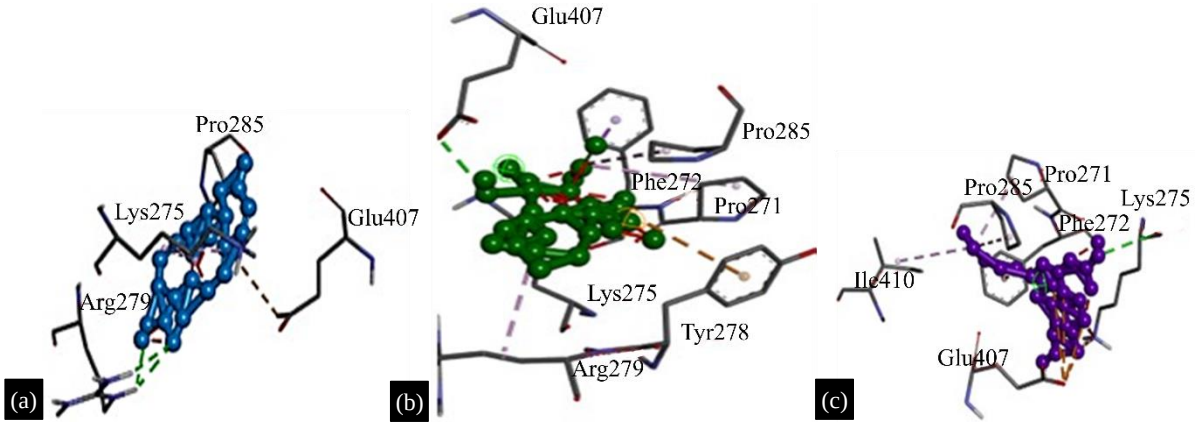

Figure 8. 3D interactions of ligands with protein PDB ID: 5KWA; (a) PubChem ID: 101607489, (b) PubChem ID: 2751795, (c) PubChem ID: 11485584 interacting with target protein of PDB ID: 5KWA.

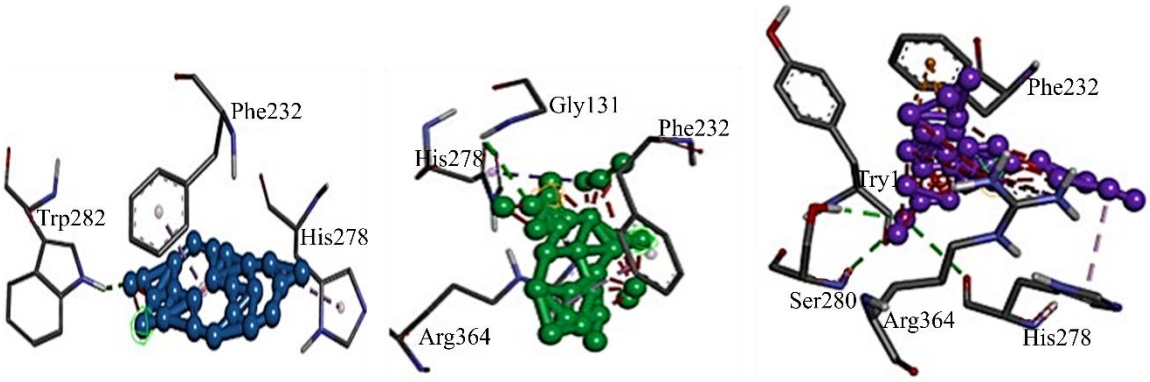

Figure 9. 3D interactions of ligands with protein PDB ID: 3ZXR. (a)PubChem ID: 101607489, (b) PubChem ID: 2751795, (c) PubChem ID: 11485584 interacting with target protein of PDB ID: 3ZXR.

ADMET Screening Results

Following visualization, an ADMET analysis is conducted that encounters significant roles in drug discovery and development, this comprehends and interprets the physiochemical properties, medicinal chemistry properties, absorption and distribution properties as well as toxicity. All of that is

accomplished using a web application called ADMET LAB 2. 0 and the results are reported in the below-mentioned (Tables 3, 4, 5, 6, and 7).

Physiochemical Property

The physicochemical parameters of the top ligands are enlisted in Tables 3 and 4.

Table 3. Physiochemical properties of top 13 ligands.

PubChem ID	MW	nHA	nHD	nHet	nRot	nRing
101607489	302.22	2	1	2	1	4
2751795	332.2	4	3	4	1	3
11485584	372.25	6	2	6	8	1
5281879	494.12	10	4	10	5	5
5471129	676.24	15	8	15	9	5
5280443	270.05	5	3	5	1	3
5281614	286.05	6	4	6	1	3
440735	288.06	6	4	6	1	3
5280445	286.05	6	4	6	1	3
128861	287.06	6	5	6	1	3
5281605	270.05	5	3	5	1	3
5281607	254.06	4	2	4	1	3
636489	328.13	5	0	5	3	3

Table 4. Physiochemical properties of top 13 ligands (Contd.).

PubChem ID	LogS	LogD	LogP	MaxRing	TPSA	Flex
101607489	-4.328	4.192	4.302	15	37.3	0.05
2751795	-4.25	3.453	4.699	14	77.76	0.059
11485584	-4.566	2.517	3.752	12	93.06	0.571
5281879	-4.388	2.826	3.597	10	148.05	0.172
5471129	-3.781	2.066	1.587	10	238.2	0.29
5280443	-3.606	2.704	3.307	10	90.9	0.056
5281614	-3.704	2.043	2.428	10	111.13	0.056
440735	-3.827	2.307	2.118	10	107.22	0.056
5280445	-3.629	2.361	2.902	10	111.13	0.056
128861	-3.432	2.83	2.895	10	112.45	0.059
5281605	-3.441	2.248	3.215	10	90.9	0.056
5281607	-3.506	2.947	3.58	10	70.67	0.056
636489	-3.705	1.648	2.421	13	69.67	0.15

MW: molecular weight; nHA: number of hydrogen bond acceptors; nHD: number of hydrogen bond donors; nHet: Number of heteroatoms; nRot: Number of rotatable bonds; nRing: Number of rings; LogS: The logarithm of aqueous solubility value; LogD: The logarithm of the n-octanol/water distribution coefficients at pH=7.4; LogP: The logarithm of the n-octanol/water distribution coefficient taken into consideration; MaxRing: Number of atoms in the biggest ring; TPSA: Topological polar surface area; Flex: Flexibility.

Medicinal Chemistry

The medicinal chemistry parameters of the top ligands are listed in Table 5.

Table 5. Medicinal chemistry properties of top 13 ligands.

PubChem ID	QED	Fsp3	PAINS	Lipinski	SAScore
101607489	0.689	0.85	0	Accepted	5.697
2751795	0.519	0.65	1	Accepted	3.928
11485584	0.502	0.9	0	Accepted	4.158

5281879	0.325	0.192	0	Accepted	3.646
5471129	0.14	0.485	0	Rejected	4.912
5280443	0.632	0	0	Accepted	2.253
5281614	0.511	0	1	Accepted	2.359
440735	0.599	0.133	1	Accepted	2.994
5280445	0.511	0	1	Accepted	2.42
128861	0.347	0	1	Accepted	3.038
5281605	0.591	0	1	Accepted	2.249
5281607	0.7	0	0	Accepted	2.096
636489	0.576	0.421	0	Accepted	4.792

QED: a measure of drug-likeness based on the concept of desirability; **Fsp3:** the number of sp3 hybridized carbons/total carbon count; **PAINS:** Pan Assay Interference Compounds; **Lipinski Rule:** Molecular weight less than 500 daltons, nHD<5, nHA<10, lipohilicity<4.15 and TPSA: 40-130 $Å^2$; **SAScore:** Synthetic accessibility score were accounted.

Absorption Properties

The absorption parameters of the top ligands are listed in Table 6.

Table 6. Absorption properties of top 13 ligands

PubChem ID	Pgp-inh	Pgp-sub	Caco-2	HIA	MDCK	F(30%)
101607489	0.001	0	-5.158	0.005	1.46E-05	0.083
2751795	0.137	0.001	-4.801	0.026	1.92E-05	0.037
11485584	0.975	0.982	-4.717	0.031	8.17E-05	0.984
5281879	0.956	0.056	-5.161	0.263	1.85E-05	0.953
5471129	0.023	0.998	-6.178	0.883	7.67E-05	0.992
5280443	0.004	0.82	-4.847	0.015	1.16E-05	0.999
5281614	0.005	0.008	-4.987	0.009	9.79E-06	0.994
440735	0.007	0.001	-5.189	0.077	6.05E-06	0.999
5280445	0.004	0.274	-5.028	0.047	1.00E-05	1
128861	0.012	0.022	-5.344	0.028	7.13E-06	0.998
5281605	0.068	0.157	-4.981	0.018	1.26E-05	0.999
5281607	0.003	0.869	-4.874	0.012	1.33E-05	0.999
636489	0.01	0.005	-4.847	0.009	2.06E-05	0.004

Pgp-inh: P-glycoprotein inhibitor Pgp-sub: P-glycoprotein substrate; Caco-2: Caco-2 Permeability; HIA: Human intestinal absorption; MDCK: Madin−Darby Canine Kidney cells (MDCK) Permeability; F(30%): the human oral bioavailability 30%.

Toxicity Properties

The toxicity parameters of the top ligands are listed in Table 7.

Table 7. Toxicity properties of top 13 ligands.

PubChem ID	DILI	AMES	hERG	Carcinogenicity	FDAMDD	IGC50	LC50
101607489	0.012	0.011	0.005	0.07	0.325	3.96	4.404
2751795	0.318	0.054	0.003	0.084	0.45	5.044	5.677
11485584	0.024	0.007	0.007	0.51	0.937	4.438	2.743
5281879	0.8	0.301	0.089	0.045	0.9	4.816	6.473
5471129	0.985	0.729	0.013	0.293	0.006	3.957	5.858
5280443	0.854	0.475	0.057	0.277	0.433	4.588	5.208
5281614	0.978	0.73	0.043	0.147	0.259	4.714	5.305
440735	0.923	0.577	0.045	0.395	0.424	4.872	5.983
5280445	0.905	0.536	0.064	0.095	0.741	4.432	5.222

128861	0.969	0.607	0.085	0.069	0.811	4.798	5.37
5281605	0.958	0.497	0.044	0.318	0.084	4.016	4.767
5281607	0.869	0.559	0.037	0.317	0.424	4.348	5.066
636489	0.884	0.008	0.001	0.087	0.085	3.889	4.89

DILI: Drug-induced liver injury; AMES: The Ames test for mutagenicity; hERG: The human ether-a-go-go related gene; FDAMDD: The maximum recommended daily dose, carcinogenicity, and 96-hour fathead minnow LC_{50} were examined; BBB: Blood–brain barrier; PPB: Plasma protein binding; VDss: Volume Distribution; Fu: fraction unbound in plasma.

Distribution Properties

The distribution parameters of the top ligands are listed in Table 8.

Table 8. Distribution Parameters of top 13 ligands.

PubChem ID	BBB	PPB	VDss	Fu
101607489	0.068	96.86%	0.719	4.89%
2751795	0.094	99.75%	2.677	2.10%
11485584	0.393	88.53%	0.832	6.03%
5281879	0.003	91.19%	0.71	13.24%
5471129	0.161	64.82%	0.772	24.98%
5280443	0.012	97.25%	0.51	3.67%
5281614	0.009	97.04%	0.477	5.17%
440735	0.023	93.32%	0.561	6.16%
5280445	0.009	95.44%	0.533	5.98%
128861	0.011	95.43%	0.609	5.63%
5281605	0.013	98.99%	0.436	4.59%
5281607	0.02	98.03%	0.493	2.78%
636489	0.038	91.01%	0.853	6.51%

DISCUSSION

The exact etiology of tuberculosis (TB), one of the most prevalent bacterial disease-related causes of fatality is *Mycobacterium tuberculosis*. Accordance to the WHO, 10 million individuals globally have chronic TB infection each year, while there were 1.4 million deaths from the ailment in 2019 (WHO). All such countries had the greatest possible MTB prevalence estimates: India (26%), Indonesia (8.5%), China (8.4%), the Philippines (6.0%) and Pakistan (5.7%). The probability of coinfection with MTB is substantially increased by several ongoing viral infections as well such as HIV, hepatitis B virus (HBV), and cytomegalovirus (CMV), which together aggravate disease severity, hasten pathogenesis, and dramatically reduce survival [19].

M. tuberculosis is an opportunistic human pathogen that relies on infection development for propagation and lacks an ambient reservoir. We hypothesize that M. tuberculosis, which is phylogenetically identical and is isolated in chronic TB cases, acquires mechanisms to avoid cytosolic detection, thereby limiting the overall secretion of cytokines by the host genome. As a corollary, M. tuberculosis would strike a delicate balance between inflicting suffering on the host (virulence) versus seeking a possibility to spread (transmission) [20].

Even though the existing “relatively brief” 6-month immunotherapy for TB is very impactful, the necessity for such a long and tedious course of medication is caused primarily by an inhabitant of metabolically amended anaerobic bacteria generally regarded as “persisters” including one that exemplifies little no replication. MTB causative agents show “antibiotic resistance” to the bactericidal medication isoniazid (INH), which mostly disrupts the mycolic acid synthesis pathways, however, inoculating medicines notably rifampin and pyrazinamide seem to be more fruitful to accomplish this. The molecular procedures implementing the longevity of MTB are nevertheless largely a mystery [21].

People are more vulnerable to and the administration of therapeutic interventions contributes to the emergence of comprehensively multi-drug resistance TB, sustained propagation, prolonged hospitalization, and death. A certain extensive and arduous protocol creates immense difficulty for clinical concordance and appropriate antibiotic availability, resulting in a key contributing factor about whether TB persists as a worldwide health concern [22].

Throughout this research, 50 bioactive diverse, and vibrant phytocompounds and their derivatives were taken into account.

For both in vivo and in vitro environments, individual species and their phytochemicals do provide intended responses against the pathogenic disease determinants. Plant-derived pharmaceuticals were demonstrated to be the healthiest mycobacteria-inhibitory therapies, with minimal or zero health consequences, facilitating the sufferers' rehabilitation. Phytoconstituents have indeed been administered as an accessible source of antioxidants and utilized raw for microbial or fungi infections since antiquity.

Alkaloids and polyphenols, constituting the 50 bioactive ligands that plants can incorporate, exhibit potent antimicrobial and antioxidant properties. Out of all the plant-produced active ingredients, 13 were evaluated based on their low binding constants and low RMSDs, with their 2D structures and Canonical SMILES obtained from PubChem.

To assess the multi-domain bacteriostatic activity of ligands, various mycobacterial proteins have been considered. These specific proteins play crucial roles essential for the survival of competing microbial cells and inflammation, as evidenced by their diverse 3D structures sourced from the well-established online database PDB. The proteins examined in this study include arabinosyltransferase C, protein kinase A, proteasomal ATPase, and glutamine synthetase. Each of these proteins is responsible for executing essential cellular activities.

The four proteins are purified with extensive analysis using BIOVIA to ensure proper and unique findings. With the assistance of a program called PyRx, the 50 bioactive ligands were satisfactorily docked with the four different *Mycobacterium* proteins and it is interestingly seen and noted that these proteins have a similar ligand interaction of binding constant. Considering the top 13 phytocompound variants studied, three of them were re-docked to ensure accurate characteristic interpretation, satisfying binding affinity, RMSD/ub, and r/lb measurements in all four mycobacterial proteins.

The top three ligands were visualized in 3D visualizing the top 3 ligands in BIOVIA Discovery Studio, and data about interactions, bond angles, and residues of amino acids was gathered.

Additionally, the top 13 compounds undertook in silico testing to estimate their drug-likeness and ADMET attributes. The acute TSPA of 238.8 is often intended for membrane permeability when assessing the physiochemical characteristics of the top 13 bioactive ligands. Lipinski's rule of five, which stipulates that the MlogP must always be less than 4.15, the number of hydrogen bond acceptors should be fewer than 5, and the number of hydrogen bond donors must be lower than 10, the ligand's MW must have 500 databases and its molecular refractivity should range between 40 and 130 and all of the compounds have a lower SAS score, indicating that they may be simple to synthesis is therefore brought up for further examination while examining the physiochemical characteristics.

MDCK monolayers may indeed be employed to identify compounds as CNS-positive or CNS-negative relying on permeability ratios while examining the absorption characteristics and while studying the distribution properties of the top 13 ligands, the BBB (blood–brain barrier) varies around 0.1–0.44, and the LC50 value and DILI score are usually utilized to reflect an attorney's acute toxicity of the 13 ligands and aminopterin has the weakest potential for recombination.

CONCLUSION

The ligand *Ent-Beyer-15-en-19-oic acid* (PubChem ID: 101607489) exhibits the lowest binding affinity (-11.6) to the *Mycobacterium* protein, according to the aforementioned study *arabinosyltransferase C* (PDB ID: 3PTY). *Horminone* (PubChem ID: 2751795), the ligand demonstrates the lowest binding affinity (-11.7) to the *Mycobacterium* protein kinase A (PDB ID: 4OWA). *Ent-Beyer-15-en-19-oic acid* (PubChem ID: 101607489) the ligand has the weakest affinity for binding (-11.6) to the *Mycobacterium* protein *proteasomal ATPase* (PDB ID: 5KWA). The *Mycobacterium* protein *glutamine synthetase* (PDB ID: 3ZXR) responds to the ligand *Ent-Beyer-15-en-19-oic acid* (PubChem ID: 101607489) with the minimum binding affinity (-13.7). Description more about relevant protein with PDB ID: 3ZXR exact understanding of biogenesis, genomic control, and cooperation in mycobacteria and other species survival in the host system might assist in the development of bioactive ingredients that have a substantial mycobacterial antagonistic effect. To learn more about these medications, in vitro research can be employed.

Acknowledgment

I extend my gratitude to BioNome in Bengaluru, India, for their Bioinformatics Training Programme, which proved instrumental in supporting my scientific research through access to computing resources. I am particularly thankful to Ms. Susha Dinesh for her invaluable assistance on the project.

Abbreviations

TB—tuberculosis
MTBC—*Mycobacterium tuberculosis* complex
Mt—*Mycobacterium tuberculosis*
PknA—protein kinase A
LAM—lipoarabinomannan
GS—glutamine Synthetase

REFERENCES

1. Kwofie SK, Adobor C, Quansah E, Bentil J, Ampadu M, Miller III WA, et al. Molecular docking and dynamics simulations studies of OmpATb identifies four potential novel natural product-derived anti-Mycobacterium tuberculosis compounds. Comput Biol Med. 2020;122:103811. doi: 10.1016/j.compbiomed.2020.103811.
2. Sudre P, Ten Dam G, Kochi A. Tuberculosis: a global overview of the situation today. Bull World Health Organ. 1992;70(2):149–59.
3. Kanabalan RD, Lee LJ, Lee TY, Chong PP, Hassan L, Ismail R et al. Human tuberculosis and Mycobacterium tuberculosis complex: a review on genetic diversity, pathogenesis and omics approaches in host biomarkers discovery. Microbiol Res. 2021;246:126674. doi: 10.1016/j.micres.2020.126674.
4. Migliori GB, Nardell E, Yedilbayev A, D'Ambrosio L, Centis R, Tadolini M et al. Reducing tuberculosis transmission: a consensus document from the World Health Organization Regional Office for Europe. Eur Respir J. 2019;53(6). doi: 10.1183/13993003.00391–2019.
5. Das N, Jena PK, Pradhan SK. Arabinosyltransferase C enzyme of Mycobacterium tuberculosis, a potential drug target: an insight from molecular docking study. Heliyon. 2020;6(2):e02693. doi: 10.1016/j.heliyon.2019.e02693.
6. Sundar S, Thangamani L, Manivel G, Kumar P, Piramanayagam S. Molecular docking, molecular dynamics and MM/PBSA studies of FDA approved drugs for protein kinase A of Mycobacterium tuberculosis; application insights of drug repurposing. Inform Med Unlocked. 2019;16:100210. doi: 10.1016/j.imu.2019.100210.
7. Wu Y, Hu K, Li D, Bai L, Yang S, Jastrab JB et al. Mycobacterium tuberculosis proteasomal ATPase Mpa has a β-grasp domain that hinders docking with the proteasome core protease. Mol Microbiol. 2017;105(2):227–41. doi: 10.1111/mmi.13695.

8. Suresh AJ, Ayyamperumal E, Pachamuthu M, Jesiya F, Surya PR. Design, synthesis, characterization and biological evaluation of some novel thiadiazole, imidazole and indole derivatives as antitubercular agents against target enzyme glutamine synthetase I. World J Pharm Pharm Sci. 2019;8(4):1601-10. doi: 10.20959/wjpps20194-13552.
9. Kim S, Chen J, Cheng T, Gindulyte A, He J, He S et al. PubChem 2019 update: improved access to chemical data. Nucleic Acids Res. 2019;47(D1):D1102–9. doi: 10.1093/nar/gky1033.
10. Kumar NP, Moideen K, Banurekha VV, Nair D, Babu S. Plasma proinflammatory cytokines are markers of disease severity and bacterial burden in pulmonary tuberculosis. Open Forum Infect Dis. 2019, July;6(7):ofz257. doi: 10.1093/ofid/ofz257.
11. Burley SK, Berman HM, Kleywegt GJ, Markley JL, Nakamura H, Velankar S. Protein Data Bank (PDB): the single global macromolecular structure archive. Methods in Molecular Biology (Clifton, N.J.); 2017. p. 627–41. doi: 10.1007/978–1–4939–7000–1_26.
12. Pawar SS, Rohane SH. Review on Discovery Studio: an important tool for molecular docking. Asian J Res Chem. 2021;14(1):1–3. doi: 10.5958/0974–4150.2021.00014.6.
13. Jamadagni SN, Godawat R, Garde S. Hydrophobicity of proteins and interfaces: insights from density fluctuations. Annu Rev Chem Biomol Eng. 2011;2:147–71. doi: 10.1146/annurev-chembioeng-061010–114156.
14. Gopalakrishnan K, Sowmiya G, Sheik SS, Sekar K. Ramachandran plot on the web (2.0). Protein Pept Lett. 2007;14(7):669–71. doi: 10.2174/092986607781483912.
15. Pagadala NS, Syed K, Tuszynski J. Software for molecular docking: a review. Biophys Rev. 2017;9(2):91–102. doi: 10.1007/s12551–016–0247–1.
16. Beg M, Athar F. Pharmacokinetic and molecular docking studies of Achyranthes aspera phytocompounds to exploring potential antituberculosis activity. J Bacteriol Mycol Open Access. 2020;8(1):18–27.
17. Siam MKS, Shohan MUS, Zafroon Z. Investigation of the anti-TB potential of selected alkaloid constituents using molecular docking approach [preprint]. BioRxiv. Cold Spring Harbor Laboratory. 2020. doi: 10.1101/2020.04.28.067090.
18. Billones JB, Carrillo MCO, Organo VG, Macalino SJY, Emnacen IA, Bernadette JBA. Virtual Screening Against Mycobacterium tuberculosisLipoate Protein Ligase B (MtbLipB)and In SilicoADMETEvaluation of Top Hits. Orient J Chem. 2013;29(4):1457–68. doi: 10.13005/ojc/290423.
19. Xu W, Snell LM, Guo M, Boukhaled G, Macleod BL, Li M et al. Early innate and adaptive immune perturbations determine long-term severity of chronic virus and Mycobacterium tuberculosis coinfection. Immunity. 2021;54(3):526–541.e7. doi: 10.1016/j.immuni.2021.01.003.
20. Sousa J, Cá B, Maceiras AR, Simões-Costa L, Fonseca KL, Fernandes AI, Ramos A, Carvalho T, Barros L, Magalhães C, Chiner-Oms Á, Machado H, Veiga MI, Singh A, Pereira R, Amorim A, Vieira J, Vieira CP, Bhatt A, Rodrigues F, Rodrigues PNS, Gagneux S, Castro AG, Guimarães JT, Bastos HN, Osório NS, Comas I, Saraiva M. Mycobacterium tuberculosis associated with severe tuberculosis evades cytosolic surveillance systems and modulates IL-1β production. Nat Commun. 2020 Apr 23;11(1):1949. doi: 10.1038/s41467–020–15832–6.
21. Dutta NK, Klinkenberg LG, Vazquez MJ, Segura-Carro D, Colmenarejo G, Ramon F et al. Inhibiting the stringent response blocks Mycobacterium tuberculosis entry into quiescence and reduces persistence. Sci Adv. 2019;5(3):eaav2104. doi: 10.1126/sciadv.aav2104.
22. Gagneux S. Ecology and evolution of Mycobacterium tuberculosis. Nat Rev Microbiol. 2018;16(4):202–13. doi: 10.1038/nrmicro.2018.8.

